数理解析研究所講究録
第824巻 1993年 255-267

STRUCTURE OF NORMAL SHOCK WAVES

Taku Ohwada

京大・工　　大和田　拓

Department of Aeronautical Engineering, Kyoto University

Kyoto 606-01, Japan

Abstract

The structure of normal shock waves is investigated numerically on the basis of the standard Boltzmann equation for hard-sphere molecules. The velocity distribution function as well as the macroscopic quantities are obtained accurately by a finite difference method where the collision term is computed directly without using the Monte-Carlo technique. The results are compared with the analytical solution for weak shock, Mott-Smith solution, and direct simulation Monte-Carlo result.

I. Introduction

The structure of normal shock waves is one of the most fundamental problems of the nonlinear Boltzmann equation. This problem has also been used by various authors as a test case of several methods and models (e.g. Refs. 1-10) and the standard solution based on the full Boltzmann equation gives useful information in the quantitative validation of them. Recently, a numerical method of the Boltzmann equation for hard-sphere molecules has been proposed and the accurate solution has been obtained.[11] In the present paper, the numerical method is described briefly and the supplementary results are shown.

II. Problem and notations

We investigate the structure of a stationary normal shock wave in a hard-sphere molecular gas. The flow is in the X_1 direction, where X_i are the space rectangular coordinates. The ρ_0, U_0, T_0, and $M = (5kT_0/3m)^{-1/2}U_0$ are the density, flow speed, temperature,

and Mach number of the gas at upstream ($X_1 = -\infty$), respectively, where k and m are the Boltzmann constant and mass of the molecule, respectively; $X_i = (\sqrt{\pi} l_0/2)x_i$; l_0 is the mean free path of gas molecules at upstream (for a hard-sphere molecular system, $l_0 = [\sqrt{2}\pi\sigma^2(\rho_0/m)]^{-1}$, where σ is the diameter of molecule); $(2kT_0/m)^{1/2}\zeta_i$ is the molecular velocity; $\rho_0(2\pi kT_0/m)^{-3/2}f(x_i, \zeta_i)$ is the velocity distribution function of the gas molecules; $\rho_0\rho$, $(2RT_0)^{1/2}u_1$, T_0T, p_0P, $p_0(P\delta_{ij} + P_{ij})$, and $p_0(2kT_0/m)^{1/2}Q_i$ are the density, flow velocity, temperature, pressure, stress tensor, and heat flow vector of the gas, respectively, where δ_{ij} is the Kronecker delta.

III. Formulation

The nondimensional Boltzmann equation in the present case is written as

$$\zeta_1 \frac{\partial f}{\partial x_1} = G[f, f] - \nu[f]f, \tag{1}$$

$$G[f,g](x_1, \zeta_i) = \int f(x_1, \zeta_i + \alpha_i(V_j\alpha_j))g(x_1, \xi_i - \alpha_i(V_j\alpha_j)) \times B(|V_j\alpha_j|, V)d\Omega(\alpha_i)d\xi_1 d\xi_2 d\xi_3, \tag{2}$$

$$\nu[f](x_1, \zeta_i) = \int f(x_1, \xi_i)B(|V_i\alpha_i|, V)d\Omega(\alpha_i)d\xi_1 d\xi_2 d\xi_3, \tag{3}$$

where $V_i = \xi_i - \zeta_i$, $V = |V_i|$, α_i is a unit vector, $d\Omega(\alpha_i)$ is the solid angle element in the direction of α_i, and B is given by

$$B(|V_i\alpha_i|, V) = \frac{1}{4\sqrt{2}\pi^2}|V_i\alpha_i|, \tag{4}$$

for hard-sphere molecules. The domain of the integration with respect to ζ_i and α_i is the whole space and all direction.

The nondimensional macroscopic variables are given by the moments of f:

$$\rho = \frac{1}{\pi^{3/2}} \int f d\zeta_1 d\zeta_2 d\zeta_3, \tag{5a}$$

$$u_i = \frac{1}{\pi^{3/2}\rho} \int \zeta_i f d\zeta_1 d\zeta_2 d\zeta_3, \tag{5b}$$

$$T = \frac{2}{3\pi^{3/2}\rho} \int (\zeta_j - u_j)^2 f d\zeta_1 d\zeta_2 d\zeta_3, \tag{5c}$$

$$P = \rho T, \tag{5d}$$

$$P_{ij} = \frac{2}{\pi^{3/2}} \int (\zeta_i - u_i)(\zeta_j - u_j) f d\zeta_1 d\zeta_2 d\zeta_3 - P\delta_{ij}, \tag{5e}$$

$$Q_i = \frac{1}{\pi^{3/2}} \int (\zeta_i - u_i)(\zeta_j - u_j)^2 f d\zeta_1 d\zeta_2 d\zeta_3. \tag{5f}$$

The boundary condition at upstream and downstream is

$$\begin{aligned} f &\to \exp[-(\zeta_1 - \sqrt{5/6}\mathrm{M})^2 - \zeta_2^2 - \zeta_3^2] \qquad (\mathrm{x}_1 \to -\infty), \\ f &\to \rho_d T_d^{-3/2} \exp[-\{(\zeta_1 - \mathrm{u_d})^2 + \zeta_2^2 + \zeta_3^2\}/\mathrm{T_d}] \qquad (\mathrm{x}_1 \to \infty), \end{aligned} \tag{6}$$

where ρ_d, u_d, and T_d are given by the Rankine-Hugoniot relation†:

$$\begin{aligned} \rho_d &= 4M^2/(M^2+3), \\ u_d &= \sqrt{5/96}(M^2+3)/M, \\ T_d &= (5M^2-1)(M^2+3)/16M^2. \end{aligned} \tag{7}$$

IV. Numerical method

The distribution function in the form of $f = f(x_1, \zeta_1, \zeta_r)$, $\zeta_r = (\zeta_2^2 + \zeta_3^2)^{1/2}$, is compatible with the present problem. We solve the Boltzmann equation (1) for $f(x_1, \zeta_1, \zeta_r)$ numerically by an iterative finite difference scheme. In this scheme, the $\partial f/\partial x_1$ term is replaced by the standard central finite difference and the collision term is computed directly using the *numerical kernel* in the following way. Let $\zeta_1^{(i)}$ be the lattice point of ζ_1 and $\zeta_r^{(j)}$ be that of ζ_r. We first expand f in terms of ζ_1 in a similar way to the finite element method:

$$f(\zeta_1, \zeta_r) = \sum_{i=-N_m}^{N_p} f(\zeta_1^{(i)}, \zeta_r) \Psi_i(\zeta_1), \tag{8}$$

where the set of basis function $\Psi_i(\zeta_1)$ is chosen in such a way that f is approximated by a sectionary quadratic function of ζ_1 which takes the exact values at $\zeta_1 = \zeta_1^{(i)}$ (here

† Equation (7) is also derived from the conservation law of the Boltzmann equation (1).

and below the space variable x_1 is omitted for short). Next, we expand $f(\zeta_1^{(i)}, \zeta_r)$ by the sequence of the Laguerre polynomials of ζ_r^2:

$$f(\zeta_1^{(i)}, \zeta_r) = \sum_{j=0}^{H-1} a_{ij} L_j(\zeta_r^2) \exp(-\zeta_r^2/2), \tag{9}$$

where $L_j(x)$ is the Laguerre polynomial of degree j. The expansion coefficient a_{ij} is given by

$$a_{ij} = 2 \int_0^\infty f(\zeta_1^{(i)}, \zeta_r) L_j(\zeta_r^2) \zeta_r \exp(-\zeta_r^2/2) \mathrm{d}\zeta_r. \tag{10}$$

We introduce ζ_r lattice system defined by $L_H[(\zeta_r^{(j)})^2] = 0$ and compute a_{ij} from the values of $f(\zeta_1^{(i)}, \zeta_r^{(k)}) \exp[(\zeta_r^{(k)})^2/2]$, $k = 1, \cdots, H$, using Gauss-Laguerre quadrature. Combining Eqs. (8) and (9) and arranging the result in the order of power of ζ_r, i.e.,

$$f(\zeta_1, \zeta_r) = \sum_{i=-N_m}^{N_p} \sum_{j=0}^{H-1} A_{ij} \Psi_i(\zeta_1) \zeta_r^{2j} \exp(-\zeta_r^2/2), \tag{11}$$

and substituting Eq. (11) into Eqs. (2) and (3), we have

$$G[f, f](\zeta_1 = \zeta_1^{(i)}, \zeta_r = \zeta_r^{(j)}) = \sum_{p=-N_m}^{N_p} \sum_{q=-N_m}^{N_p} \sum_{a=0}^{H-1} \sum_{b=0}^{H-1} \Omega_{pqab}^{ij} A_{pa} A_{qb}, \tag{12}$$

$$\nu[f](\zeta_1 = \zeta_1^{(i)}, \zeta_r = \zeta_r^{(j)}) = \sum_{p=-N_m}^{N_p} \sum_{a=0}^{H-1} \Lambda_{pa}^{ij} A_{pa}, \tag{13}$$

where

$$\Omega_{pqab}^{ij} = G[\Psi_p(\xi_1) \xi_r^{2a} E_r, \Psi_q(\xi_1) \xi_r^{2b} E_r](\zeta_1 = \zeta_1^{(i)}, \zeta_r = \zeta_r^{(j)}), \tag{14}$$

$$\Lambda_{pa}^{ij} = \nu[\Psi_p(\xi_1) \xi_r^{2a} E_r](\zeta_1 = \zeta_1^{(i)}, \zeta_r = \zeta_r^{(j)}), \tag{15}$$

with

$$E_r = \exp(-\xi_r^2/2).$$

The complexity of the collision term appears only in the numerical kernel Ω_{pqab}^{ij} and Λ_{pa}^{ij}, which can be computed in advance and are stored. In order to reduce the number of elements of numerical kernel, a uniform ζ_1 lattice system is introduced, i.e., $\zeta_1^{(i)} = i\Delta$.

Then, from the relation of the collision operator for the translation and mirror image, we have

$$\Omega^{ij}_{pqab} = \Omega^{0,j}_{p-i,q-i,ab}, \qquad \Lambda^{ij}_{pa} = \Lambda^{0,j}_{p-i,a}, \tag{16}$$

$$\Omega^{0,j}_{pqab} = \Omega^{0,j}_{-p,-q,ab}, \qquad \Lambda^{0,j}_{pa} = \Lambda^{0,j}_{-p,a}. \tag{17}$$

Furthermore, for hard-sphere molecules the following relation holds:

$$\Omega^{0,j}_{pqab} = \Omega^{0,j}_{qpba}, \qquad \Omega^{0,j}_{pqab} = \Omega^{0,j}_{pqba}. \tag{18}$$

Owing to Eqs. (16)-(18) we can reduce the total number of the elements from $(N_m + N_p + 1)^3 H^3$ to about $(3/8)(N_m + N_p + 1)^2 H^3$. Each element of the numerical kernel, generally expressed by a five fold integral, can be reduced to two fold one in the case of hard-sphere molecules and is computed accurately.[11]; if we expand f in terms of ζ_r by a set of basis function, the effective domain of integration of the numerical kernel becomes geometrically very complicated.

The present method is based on the form of the similarity solution (see Ref. 12 for the linearized Boltzmann equation). The numerical kernel method for general form of the distribution function, though the lattice system which can be used in the actual computation is limited to very coarse one at the present stage, has been proposed by Tan, et. al in Ref. 13.

V. Result and discussion

In Ref. 11, the numerical results are presented for $M = 1.2 \sim 3$ together with several accuracy data of computation. In the present study, we supplement the results for $M =$ 1.1 and 3.2.

The computation was carried out using the numerical kernel in Ref. 11 [(M3) molecular velocity lattice system, i.e., 101 lattice points for ζ_1 ($\Delta = 0.15$) and 14 lattice points for ζ_r ($H = 14$, $\zeta_r^{(H)} = 6.6607\ldots$)]. In the case of $M = 1.1$, we computed $\bar{f}(x_1, \zeta_1, \zeta_r) = f(x_1, \zeta_1/\sqrt{2}, \zeta_r/\sqrt{2})$ in stead of f, since the distribution function is almost upstream

Maxwellian, i.e., $f(x_1, \zeta_1, \zeta_r) \sim \exp(-\zeta_1^2 - \zeta_r^2)$, and therefore, $\bar{f} \sim \exp[-\zeta_r^2/2]$, and the leading term of the Laguerre polynomial expansion is proportional to $\exp[-\zeta_r^2/2]$. The space interval is $-70 \leq x_1 \leq 70$ for $M = 1.1$ and $-20 \leq x_1 \leq 20$ for $M = 3.2$. The space lattice system is uniform for $M = 1.1$ (100 sections) and nonuniform for $M = 3.2$ [(S2) system in Ref. 11, i.e., 100 sections with the minimum width 0.100 around $x_1 = 0$ and maximum one 1.283 around $x_1 = \pm 20$]. The numerical results satisfy the conservation law, the constancy of mass, moment, and energy fluxes at all the space lattice points, within the range of 0.03% for $M = 1.1$ and 0.05% for $M = 3.2$. For the comparison, we also carried out the Monte-Carlo direct simulation using Bird's NTC method and the piston boundary condition at down stream[8] [Hard-Sphere, $M = 3.2$, $-20 \leq x_1 \leq 20$, 100 uniform cells, about 32500 particles, 8000 samples].

The ρ, u_1, and T vs. x_1 for $M = 1.1$ are tabulated in Table I together with those of the asymptotic solution for weak shock[11], which is derived up to $O(\epsilon^2)$, $(\epsilon = M - 1)$, by the ϵ expansion of f around upstream Maxwellian under the assumption that the shock thickness is $O(l_0/\epsilon)$ [see Appendix]. The present numerical result agrees very well with the asymptotic solution. The normalized density $\tilde{\rho} = \rho/(\rho(\infty) - 1)$, flow speed $\tilde{u}_1 = u_1/(u_1(-\infty) - u_1(\infty))$, and temperature $\tilde{T} = T/(T(\infty) - 1)$ vs. x_1 for $M = 3.2$ are plotted in Fig.1 together with the Mott-Smith solution corresponding to the moment equation of $\int \zeta_1^3 f d\zeta_1 \zeta_2 \zeta_3$ and the DSMC result. In Fig.2 the results of these methods are compared at the distribution function level. Although the difference between the Mott-Smith solution and the present result is slight at the macroscopic level, there is a distinct difference at the microscopic level. The standard deviation of the samples of simulation for the density is not small, nevertheless, the average of samples agrees very well with the present result at the microscopic level as well, which shows the averaging procedure works quite well.

We analyzed the structure of normal shock waves up to moderate strength numerically with good accuracy. In the case of strong shock wave (the temperature difference in the gas is large), many terms is required in the Laguerre polynomial expansion for the

accurate computation. However, it becomes very difficult to compute $\Omega^{0,k}_{pqab}$ accurately for large a and b. The application range of the present method is practically limited up to moderate shock strength.

Appendix: Analysis of weak shock waves

A. Outline of analysis

The analysis is carried out in a similar way to the Hilbert expansion.[14] We introduce a new space coordinate $\eta = \epsilon x_1$, where $\epsilon = M - 1$. For the convenience of analysis, we use the following independent variables and function: $(\hat{\zeta}_1, \hat{\zeta}_2, \hat{\zeta}_3) = (\zeta_1 - \sqrt{5/6}M, \zeta_2, \zeta_3)$, $\hat{\zeta} = (\hat{\zeta}_i^2)^{1/2}$, $\hat{f}(\eta, \hat{\zeta}_1, \hat{\zeta}_2, \hat{\zeta}_3) = f(x_1, \zeta_1, \zeta_2, \zeta_3)$. Then the Boltzmann equation (1) for $\hat{f}$ is written as

$$(\hat{\zeta}_1 + \sqrt{5/6}M)\frac{\partial \hat{f}(\eta, \hat{\zeta}_i)}{\partial \eta} = \frac{1}{\epsilon} Q[\hat{f}, \hat{f}](\eta, \hat{\zeta}_i), \tag{A1}$$

where

$$Q[\hat{f}, \hat{g}] = \frac{1}{2}(G[\hat{f}, \hat{g}] + G[\hat{g}, \hat{f}] - \nu[\hat{f}]\hat{g} - \nu[\hat{g}]\hat{f}).$$

We expand $\hat{f}$ into a power series of ϵ around the upstream Maxwellian $\hat{f}_0 = \exp(\hat{\zeta}^2)$:

$$\hat{f}(\eta, \hat{\zeta}_i) = \hat{f}_0[1 + \phi_1(\eta, \hat{\zeta}_i)\epsilon + \phi_2(\eta, \hat{\zeta}_i)\epsilon^2 + \cdots]. \tag{A2}$$

Substituting Eq.(A2) into Eq.(A1) and assuming $\partial\phi_i/\partial\eta = O(1)$, i.e., $\delta/l_0 = O(1/\epsilon)$, and arranging the result in the order of power of ϵ, we have the following sequence of linear integral equations:

$$2Q[\hat{f}_0, \hat{f}_0\phi_1] = 0, \tag{A3a}$$

$$2Q[\hat{f}_0, \hat{f}_0\phi_2] = (\hat{\zeta}_1 + \sqrt{5/6})\hat{f}_0\frac{\partial \phi_1}{\partial \eta} - Q[\hat{f}_0\phi_1, \hat{f}_0\phi_1], \tag{A3b}$$

$$\cdots\cdots\cdots\cdots\cdots\cdots,$$

$$2Q[\hat{f}_0, \hat{f}_0\phi_n] = (\hat{\zeta}_1 + \sqrt{5/6})\hat{f}_0\frac{\partial \phi_{n-1}}{\partial \eta} + \sqrt{5/6}\hat{f}_0\frac{\partial \phi_{n-2}}{\partial \eta} - \sum_{\substack{l+m=n \\ 1\le l \\ 1\le m}} Q[\hat{f}_0\phi_l, \hat{f}_0\phi_m] \quad (n \ge 3). \tag{A3c}$$

The boundary condition (16) is expanded in a similar way to Eq.(A2). The integral equations are, in principle, solved from the lowest order. The homogeneous integral equation [(A3a)] has nontrivial solutions $\{1, \hat{\zeta}_1, \hat{\zeta}^2\}$ and the coefficient functions of $\{1, \hat{\zeta}_1, \hat{\zeta}^2\}$ in ϕ_n, functions of η, are determined by the solvability conditions of $(n+1)$th and $(n+2)$th integral equations and the boundary condition for ϕ_n. The position of solution is arbitrary in this problem and we determine it in such a way that the density corresponding to $\hat{f}_0\phi_n$, $\rho^n(\eta)$, satisfies $\rho^n(0) = [\rho^n(-\infty) + \rho^n(+\infty)]/2$.

B. Result

We show the results up to $O(\epsilon^2)$ below. The distribution function is

$$\phi_1 = a(\eta)(-\sqrt{15/2}\hat{\zeta}_1 + \hat{\zeta}^2), \tag{A4a}$$

$$\begin{aligned}\phi_2 =& b_1(\eta) + b_2(\eta)\hat{\zeta}_1 + b_3(\eta)\hat{\zeta}^2 \\ &+ a(\eta)^2[-\sqrt{15/2}\hat{\zeta}_1(\hat{\zeta}^2 - 5/2) + (15/4)(\hat{\zeta}_1^2 - \hat{\zeta}^2/3) + (1/8)(4\hat{\zeta}^4 - 20\hat{\zeta}^2 + 15)] \\ &+ \sqrt{30}\lambda_1^{-1}\exp(-\sqrt{30}\eta/\lambda_1)\mathrm{a}(\eta)^2[\sqrt{15/8}(\hat{\zeta}_1^2 - \hat{\zeta}^2/3)\mathrm{B}(\hat{\zeta}) - \hat{\zeta}_1\mathrm{A}(\hat{\zeta})],\end{aligned} \tag{A4b}$$

where

$$\begin{aligned} a(\eta) =& (1 + \exp(-\sqrt{30}\eta/\lambda_1))^{-1}, \\ b_1(\eta) =& (15/2)a(\eta)[-\lambda_4 + (\lambda_4 - 1/2)a(\eta)], \\ b_2(\eta) =& \sqrt{15/2}[-b_3(\eta) + a(\eta)\{5\lambda_4 - 1 - (5\lambda_4 - 5/2)a(\eta)\}], \\ b_3(\eta) =& a(\eta)^2\left[5/2 + \exp(-\sqrt{30}\eta/\lambda_1)\{\lambda_2\eta + \lambda_3\log[1 + \exp(\sqrt{30}\eta/\lambda_1)] + \lambda_5\}\right], \end{aligned} \tag{A5}$$

$$\begin{aligned} &\lambda_1 = (2\gamma_1 + \gamma_2), \quad \lambda_2 = \sqrt{15/2}[-8(\gamma_1^2 + \gamma_2^2 - \gamma_s)/\lambda_1^3 + 1/\lambda_1], \\ &\lambda_3 = -(20\gamma_1\gamma_2 + 8\gamma_s)/\lambda_1^2 + (14\gamma_1 + 13\gamma_2 - 2\gamma_4 - \gamma_5)/\lambda_1 - 11/2, \\ &\lambda_4 = \gamma_2/\lambda_1, \quad \lambda_5 = 5\lambda_4 - \lambda_3\log 2. \end{aligned} \tag{A6}$$

The $A(\hat{\zeta})$ and $B(\hat{\zeta})$ are the solution of the following integral equations:

$$\left.\begin{aligned} &2Q[\hat{f}_0\hat{\zeta}_1 A(\hat{\zeta}), \hat{f}_0] = -\hat{f}_0\hat{\zeta}_1(\hat{\zeta}^2 - 5/2), \\ &\int_0^\infty \hat{\zeta}^4 A(\hat{\zeta})\exp(-\hat{\zeta}^2)\mathrm{d}\hat{\zeta} = 0, \end{aligned}\right\} \tag{A7}$$

$$2Q[\hat{f}_0(\hat{\zeta}_1^2 - \hat{\zeta}^2/3)B(\hat{\zeta}), \hat{f}_0] = -2\hat{f}_0(\hat{\zeta}_1^2 - \hat{\zeta}^2/3), \tag{A8}$$

and γ_i are constants given by

$$\gamma_1 = I_6(B), \qquad \gamma_2 = 2I_6(A), \qquad \gamma_3 = I_6(AB),$$
$$\gamma_4 = -(5/2)\gamma_1 + I_8(B) + (1/2)I_6(BC), \qquad \gamma_5 = -6\gamma_2 + 2I_8(A) + 2I_4(AG), \tag{A9}$$
$$\gamma_s = (5/2)I_4(A^2) + (5/4)I_6(B^2) - 2\gamma_3,$$

where

$$I_n(F) = (8/15)\pi^{-1/2}\int_0^\infty \hat{\zeta}^n F(\hat{\zeta})\exp(-\hat{\zeta}^2)\mathrm{d}\hat{\zeta},$$

and $C(\hat{\zeta})$ and $G(\hat{\zeta})$ are defined by

$$2Q[\hat{f}_0\hat{\zeta}^2, \hat{f}_0(\hat{\zeta}_1^2 - \hat{\zeta}^2/3)B(\hat{\zeta})] = \hat{f}_0(\hat{\zeta}_1^2 - \hat{\zeta}^2/3)(C(\hat{\zeta}) - 3), \tag{A10}$$

$$2Q[\hat{f}_0\hat{\zeta}^2, \hat{f}_0\hat{\zeta}_1 A(\hat{\zeta})] = \hat{f}_0[\hat{\zeta}_1 G(\hat{\zeta}) - (3/2)\hat{\zeta}_1(\hat{\zeta}^2 - 5/2)]. \tag{A11}$$

The macroscopic quantities corresponding to the above distribution function are

$$\left.\begin{aligned}
\rho &= 1 + (3/2)a(\eta)\epsilon + [b_1(\eta) + (3/2)b_3(\eta)]\epsilon^2 + \cdots, \\
u_1 &= \sqrt{5/6} + [\sqrt{5/6} - \sqrt{15/8}a(\eta)]\epsilon + [b_2(\eta)/2 + \sqrt{135/32}a(\eta)^2]\epsilon^2 + \cdots, \\
T &= 1 + a(\eta)\epsilon + [b_3(\eta) - (11/4)a(\eta)^2]\epsilon^2 + \cdots, \\
P_{11} &= -2P_{22} = -2P_{33} = 10\gamma_1\lambda_1^{-1}\exp(-\sqrt{30}\eta/\lambda_1)\mathrm{a}(\eta)^2\epsilon^2 + \cdots, \\
Q_1 &= -(5/4)\sqrt{30}\gamma_2\lambda_1^{-1}\exp(-\sqrt{30}\eta/\lambda_1)\mathrm{a}(\eta)^2\epsilon^2 + \cdots.
\end{aligned}\right\} \tag{A12}$$

The accurate numerical data of $A(\hat{\zeta})$ and $B(\hat{\zeta})$ for hard-sphere molecules were first obtained by Pekeris and Alterman[15] and the recomputed data are tabulated in Ref.16. The quantities of γ_i for hard-sphere molecules are

$$\left.\begin{aligned}
\gamma_1 &= 1.270042427, \quad \gamma_2 = 1.922284066, \quad \gamma_3 = 1.947906335, \\
\gamma_4 &= 0.635021214, \quad \gamma_5 = 0.961142033, \quad \gamma_s = 4.893662449.
\end{aligned}\right\} \tag{A13}$$

It should be noted that the above results up to $O(\epsilon^2)$ are derived from Burnett solution in Chapman-Enskog theory[17] when the macroscopic variables are expanded in a similar way.

References

[1]Mott-Smith, H.M., "The Solution of the Boltzmann Equation for a Shock Wave", Physical Review, Vol. 88, 1951, pp.885-892.

[2]Bird, G.A., "Shock-Wave Structure in a Rigid Sphere Gas", *Rarefied Gas Dynamics*, edited by de Leeuw, J.H., Academic, New York, 1965, Vol.1, pp.216-222.

[3]Anderson, D.G., "Numerical solution of the Krook kinetic equation", Journal of Fluid Mechanics, Vol.25, 1966, pp.271-287.

[4]Segal, B.M. and Ferziger, J.H., "Shock-Wave Structure using Nonlinear Model Boltzmann Equations", Physics of Fluids, Vol. 15, 1972, pp.1233-1247.

[5]Hicks, B.L., Yen, S-M., and Reilly, B.J., "The Internal Structure of Shock Waves", Journal of Fluid Mechanics, Vol. 53, 1972, pp.85-111.

[6]Aristov, V.V. and Cheremisin, F.G., "Shock wave structure in monatomic gas in the case of power-law interaction potentials", Fluid Dynamics Vol. 17, 1982, pp.964-968.

[7]Nanbu, K. and Watanabe, Y., "Analysis of internal structure of shock waves by means of the exact direct-simulation method", *Rarefied Gas Dynamics*, edited by Oguchi, H., Univ. Tokyo Press, Tokyo, 1984, pp.183-190.

[8]Bird, G.A., "Perception of Numerical Methods in Rarefied Gas Dynamics", *Rarefied Gas Dynamics: Theoretical and Computational Techniques*, edited by Muntz, E.P., Weaver, D.P., and Campbell, D.H., AIAA, Washington, DC, 1989, pp.211-226.

[9]Erwin, D.A., Pham-Van-Diep, G.C., and Muntz, E.P., "Nonequilibrium gas flows. I. : A detailed validation of Monte Carlo direct simulation for monatomic gases", Physics of Fluids A, Vol. 3, 1991, pp.697-705.

[10]Matsumoto, H. and Koura, K., "Comparison of velocity distribution functions in an argon shock wave between experiments and Monte Carlo calculations for Lennard-Jones potential", Physics of Fluids A, Vol. 3, 1991, pp.3038-3045.

[11]Ohwada, T. "Structure of normal shock wave: Direct numerical analysis of the Boltzmann equation for hard-sphere molecules", Physics of Fluids A, Vol. 5, 1993 (to be published).

[12]Sone, Y., Ohwada, T., and Aoki, K., "Temperature jump and Knudsen layer in a rarefied gas over a plane wall: Numerical analysis of the linearized Boltzmann equation for hard-sphere molecules", Physics of Fluids A, Vol. 1, 1989, pp.363-370; Ohwada, T., Sone, Y., and Aoki, K., "Numerical analysis of the shear and thermal creep flows of a rarefied gas over a plane wall on the basis of the linearized Boltzmann equation for hard-sphere molecules", Physics of Fluids A, Vol. 1, 1989, pp.1588-1599.

[13]Tan, Z-Q., Chen, Y-K., Varghese, P.L., and Howell, J.R., "New Strategy to Evaluate the Collision Integral of the Boltzmann Equation", *Rarefied Gas Dynamics: Theoretical and Computational Techniques*, ed. Muntz, E.P., Weaver, D.P., and Campbell, D.H., AIAA, Washington, DC, 1989, pp.359-373.

[14]Cercignani, C. *Theory and Application of the Boltzmann Equation*, (Scottish Academic, 1975).

[15] Pekeris, C.L. and Alterman, Z. "Solution of the Boltzmann-Hilbert integral equation II. The coefficients of viscosity and heat conduction", *Proceedings of the National Academy of Sciences of the U.S.A.* Vol. 43, 1957, pp.998-1007.

[16]Ohwada, T. and Sone, Y. "Analysis of thermal stress slip flow and negative thermophoresis using the Boltzmann equation for Hard-Sphere molecules", Eur. J. Mech., B/Fluids **11**, 1992, pp.389-414.

[17] Chapman, S. and Cowling, T.G. *The Mathematical Theoru of Non-Uniform Gases*, 2nd Ed. (Cambridge U. P., London, 1952).

Table I. The density ρ, flow velocity u_1, and temperature T vs. x_1 for $M = 1.1$.

	Numerical			Asymptotic[11]		
x_1	ρ	u_1	T	ρ	u_1	T
$-\infty$	1.000	1.004	1.000	1.000	1.004	1.000
-60	1.000	1.004	1.000	1.000	1.004	1.000
-50	1.000	1.004	1.000	1.000	1.004	1.000
-40	1.001	1.004	1.000	1.001	1.003	1.001
-30	1.003	1.001	1.002	1.003	1.001	1.003
-20	1.011	0.993	1.009	1.011	0.993	1.009
-10	1.034	0.972	1.026	1.034	0.971	1.026
0	1.075	0.934	1.054	1.075	0.934	1.055
10	1.115	0.901	1.079	1.116	0.900	1.079
20	1.137	0.883	1.091	1.138	0.883	1.091
30	1.145	0.877	1.095	1.146	0.877	1.095
40	1.148	0.875	1.097	1.149	0.875	1.097
50	1.149	0.874	1.097	1.150	0.874	1.097
60	1.150	0.873	1.098	1.150	0.874	1.097
∞	1.150	0.873	1.098	1.150	0.874	1.098

The results are shifted for x_1 in such a way that the point with average density is located at $x_1 = 0$. The data for the present numerical computation are interpolated with sufficient accuracy from those at the lattice points.

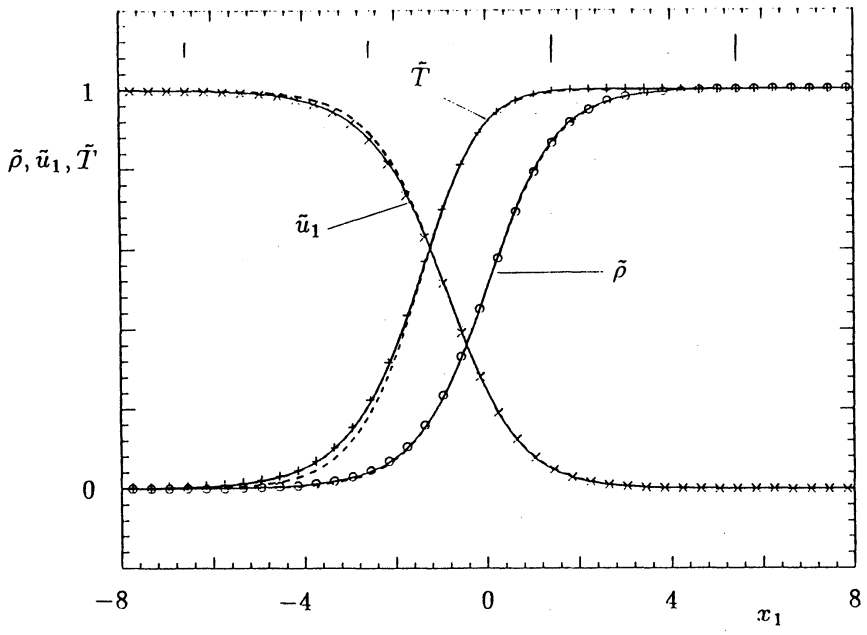

Fig.1. The profiles of normalized density $\tilde{\rho}$, flow velocity $\tilde{u}_1$, and temperature $\tilde{T}$ vs. x_1 for $M = 3.2$. Here, ———— indicates the present numerical result, – – – – – the Mott-Smith[1], and o, ×, and + are $\tilde{\rho}$, $\tilde{u}_1$, and $\tilde{T}$ of the DSMC result, respectively. The results are shifted for x_1 in such a way that the point with average density is located at $x_1 = 0$. The length of each vertical line shows the magnitude of the standard deviation of the DSMC samples for the density at the corresponding point.

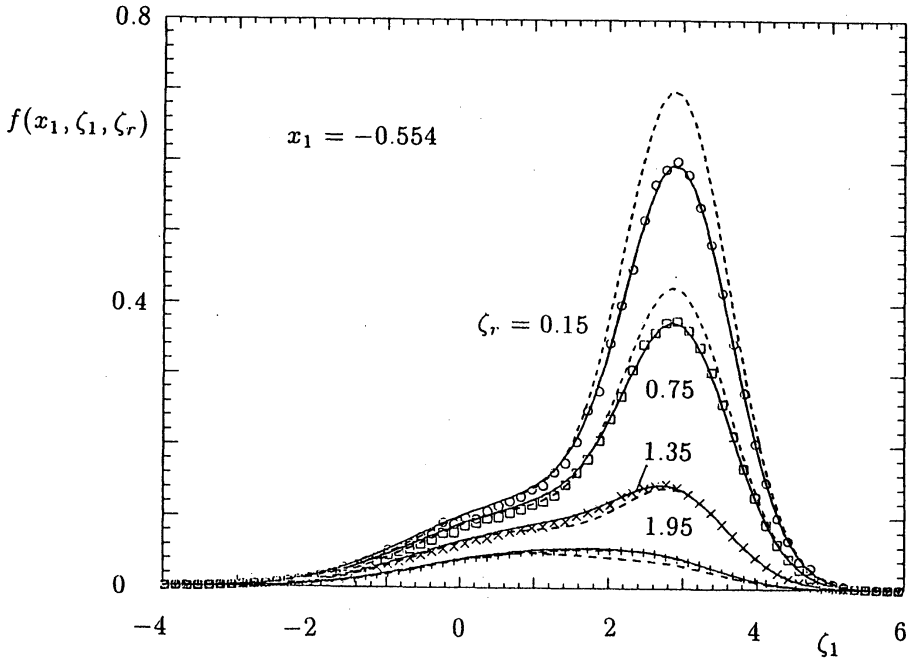

(a)

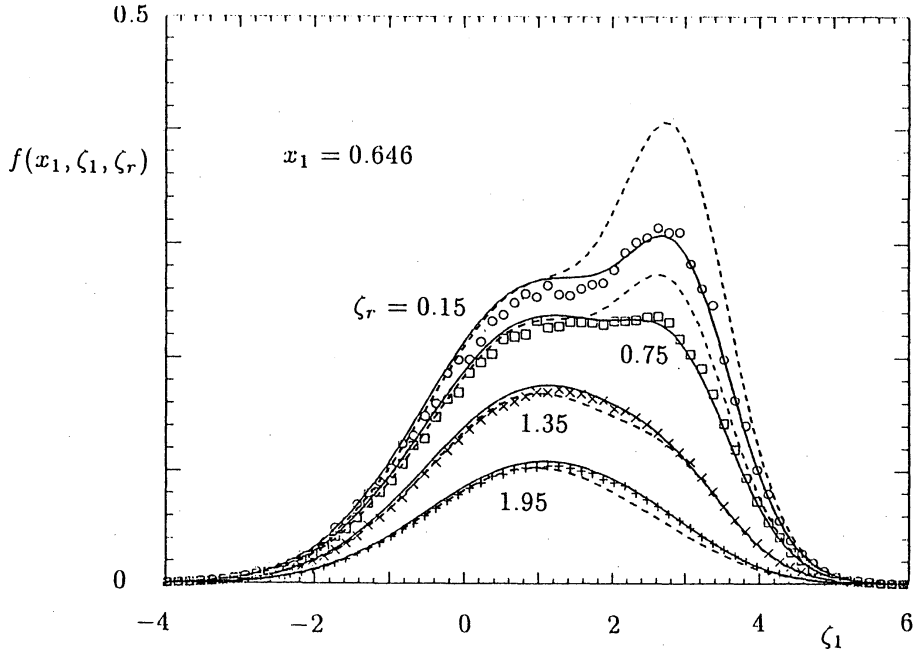

(b)

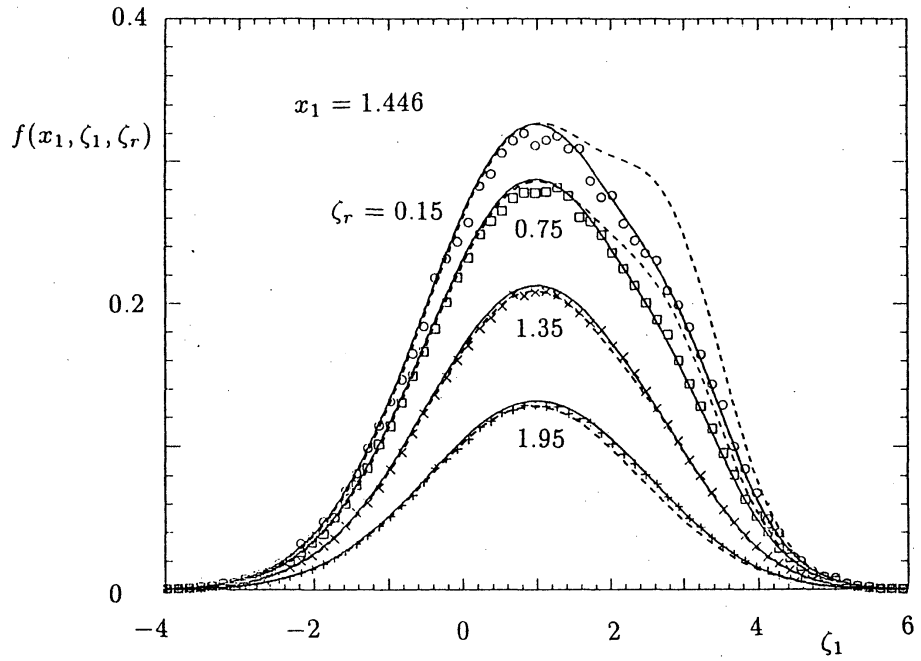

(c)

Fig.2. Comparison of the distribution function $f(x_1, \zeta_1, \zeta_r)$ for $M = 3.2$ at (a) $x_1 = -0.554$, (b) $x_1 = 0.646$, and (c) $x_1 = 1.446$. Here, ——— indicates the present numerical result, – – – – – the Mott-Smith[1], and o, □, ×, and + are the DSMC result corresponding to $\zeta_r = 0.15$, 0.75, 1.35, and 1.95, respectively. The results are shifted for x_1 in such a way that the point with average density is located at $x_1 = 0$.